International Journal of Applied Engineering Research
ISSN 0973-4562 Volume 10, Number 4 (2015) pp. 9003-9016

http://www.ripublication.com

Design of Digital Controllers For Sensorless BLDC Motor Drives

S.Vijayan
PG Student,
Department of EEE, Shanmuganathan Engineering College, Pudukkottai

Dr.A.Vanisri
Professor& Head, Department of EEE, Shanmuganathan Engineering College, Pudukkottai.

P.Senthilkumar
Assistant Professor,
Department EEE, Shanmuganathan Engineering College Pudukkottai.

Abstract

Brushless DC Servomotors and their drives are penetrating the market of home appliances, space vehicles, Robotics, HVAC Industries, and automotive applications in recent years.In such applications, conventional controllers like P, PI and PID are being used with the BLDC servomotor drive control systems to achieve satisfactory steady-state and transient state operations.However, the major problem associated with the conventional PI controller is that they do not yield better transient and steady-state responses under different operating conditions.This project describes design of fuzzy controllers for achieving improved performance of sensorless Brushless dc (BLDC) motor drives. The performance of fuzzy and PID controller-based sensorless BLDC servomotor drives is investigated under different operating conditions such as change in reference speed, parameter variations, load disturbance, etc. The position sensorless BLDC drive proposed using MATLAB/SIMULINK, is based on detection of back emf zero crossing from the terminal voltages.

Keywords: Brushless DC, Back emf, PI Controller, Fuzzy Controller, MATLAB/SIMULINK.

Introduction

Over the last few years, with continuous technology development in the power semiconductors, Microprocessors, Logic ICs, Adjustable Speed Drivers and increase

in permanent magnet brushless electric motor production has enable us the reliable and cost-effective solution for a broad range of adjustable speed applications. BLDC motors are gradually replacing dc motors and ac motors due to their high efficiency, silent operation, reliability, high operating speed, small size, low maintenance and excellent torque speed characteristics.
The BLDC motor drive system consists of a dc power supply switched to the stator phase windings of the motor through an inverter by power switching devices. The detection of rotor position will determine the switching sequence of the inverter. Three-phase inverters are generally used to control these motors, requiring a rotor position sensor for starting and providing the proper commutation sequence to stator windings. These position sensors can be hall sensors or absolute position sensors. However, the hall sensors will lose its sensing capability at the temperature above 125□C. therefore hall sensors are not feasible in high temperature conditions. The drawbacks of sensored motor control system are not increased cost and size of the motor, and need special mechanical arrangement for mounting the sensors. Another major problem is associated with the conventional controllers pose difficulties under the conditions of nonlinearity, load disturbances, and parameter variations. So an attempt is made to remove the drawbacks associated with sensored control and the use of traditional controllers by using sensorless control and fuzzy controller for PMBLDC motor.

Modeling of Bldc Motor

The BLDC servomotor drive system consisting of BLDC servomotor and IGBT inverter is modeled based on the assumptions that all stator phase windings have equal resistance per phase, constant self and mutual inductances; power semiconductor switches are ideal; iron losses are negligible; and the motor is unsaturated.The equivalent circuit of the BLDC servomotor drive system is shown.

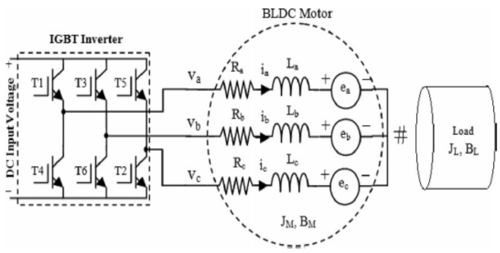

Figure 2.1: Modeling of BLDC servomotor

The line to line voltage equations are expressed in matrix form as

$$\begin{bmatrix} Vab \\ Vbc \\ Vca \end{bmatrix} = \begin{bmatrix} R & -R & 0 \\ 0 & R & -R \\ -R & 0 & R \end{bmatrix} \begin{bmatrix} ia \\ ib \\ ic \end{bmatrix} + \begin{bmatrix} L-M & M-L & 0 \\ 0 & L-M & M-L \\ M-L & 0 & L-M \end{bmatrix} X \frac{dia}{dt} \begin{bmatrix} ia \\ ib \\ ic \end{bmatrix} + \begin{bmatrix} ea-eb \\ eb-ec \\ ec-ea \end{bmatrix} \tag{2.1}$$

Since mutual inductance is negligible as compared to the self-inductance, the above equation can be rewritten as

$$\begin{bmatrix} Vab \\ Vbc \\ Vca \end{bmatrix} = \begin{bmatrix} R & -R & 0 \\ 0 & R & -R \\ -R & 0 & R \end{bmatrix} \begin{bmatrix} ia \\ ib \\ ic \end{bmatrix} + \begin{bmatrix} L & -L & 0 \\ 0 & L & -L \\ -L & 0 & L \end{bmatrix} X \frac{dia}{dt} \begin{bmatrix} ia \\ ib \\ ic \end{bmatrix} + \begin{bmatrix} ea - eb \\ eb - ec \\ ec - ea \end{bmatrix} \quad (2.2)$$

Where L and M are self-inductance and mutual inductance per phase; R is the stator winding resistance per phase; e_a,e_b and e_c are the back EMFs of phases a, b and c respectively; i_a,i_b,andi_c are the phase currents of phase a, b and c respectively.
The electromagnetic torque developed by the motor can be expressed as

$$T_e = (e_a i_a + e_b i_b + e_c i_c)/\omega$$
$$= K_t I \quad (2.3)$$

Where i_a=i_b=i_c=I, ω is the angular velocity in radians per second, and K_t is the torque constant.
Since the electromagnetic torque is utilized to overcome the opposing torques of inertia and load, it can also be written as

$$T_e = T_L + Jm\frac{d\omega}{dt} + Bm\omega \quad (2.4)$$

Where T_L is the load torque, J_m is the inertia, and B_m is the friction constant of the BLDC servomotor.
The load torque can be expressed in terms of load inertia JL and friction BL components as

$$T_L = JL\frac{d\omega}{dt} + BL\omega \quad (2.5)$$

The output power developed by the motor is

$$P = T_e\omega \quad (2.6)$$

$$E = e_a = e_b = e_c = K_b\omega \quad (2.7)$$

Where K_b is back EMF constant, E is back EMF per phase, and ω is angular velocity in radians per second.
The parameters of motor are phase resistance, phase inductance, and inertia and friction of BLDC servomotor and load. It is necessary to determine the parameters of both BLDC servomotor and load so as to design conventional controllers like P, PI, and PID controllers.
The parameters that are likely to vary during the working conditions are R, J_m, J_L, B_M and B_L. These parameters can influence the speed response of the BLDC servomotor drive system. The decrease in the values of power consuming friction components B_m and B_L will increase the deceleration time of the speed response vice versa.Another parameter, which is likely to vary during working conditions is phase resistance of the BLDC servomotor due to addition of terminal resistance, change in resistance of phase winding, and change in on-state resistance of Insulated Gate Bipolar Transistor switches due to change in temperature. The change in phase resistance can also affect the speed response of BLDC servomotor drive system. Mixed combination of inertia, friction, and phase resistance of the BLDC servomotor may lead to large overshoots that are undesirable in most of the control applications. Therefore, the BLDC

servomotor drive system needs suitable controllers such as PID or fuzzy controllers to speed up the response, reduce overshoot, and steady-state error to meet up the application requirements.

B.Proposed Sensorless Speed Control

Consider a BLDC motor having three stator phase windings connected in stator. Permanent magnets are mounted on the rotor. The BLDC motor is driven by a three phase inverter in which the device are triggered with respect to the rotor position as shown in fig 3.2 The phase A terminal voltage with respect to the star point of the stator V_{an} is given as

$$V_{an} = R_a i_a + L_a \frac{dia}{dt} + e_{an} \tag{2.8}$$

Where R_a is the stator resistance, L_a is the phase inductance, e_{an} is the back EMF, and $i_a$is the phase current of phase A.

Similar equations can be written for the other two phases, are

$$V_{bn} = R_b i_b + L_b \frac{dib}{dt} + e_{bn} \tag{2.9}$$

$$V_{cn} = R_c i_c + L_c \frac{dic}{dt} + e_{cn} \tag{2.10}$$

Where the symbols have their obvious meanings. From this, line voltage V_{ab} may be determined as

$$V_{ab} = V_{an} - V_{bn}$$

$$= R(i_a - i_b) + L \frac{d(ia-ib)}{dt} + e_{an} - e_{bn} \tag{2.11}$$

Similarly

$$V_{bc} = R(i_b - i_c) + L \frac{d(ib-ic)}{dt} + e_{bn} - e_{cn} \tag{2.12}$$

$$V_{ca} = R(i_c - i_a) + L \frac{d(ic-ia)}{dt} + e_{cn} - e_{an} \tag{2.13}$$

These line voltage can, however, be estimated without the need for star point by taking the difference of terminal voltages measured with respect to the negative dc bus.

Subtracting (4) from (5) gives

$$V_{abbc} = R(i_a - 2i_b + i_c) + L \frac{d(ia-2ib+ic)}{dt} + e_{an} - 2e_{bn} + e_{cn} \tag{2.14}$$

Consider the interval phase A and C are conducting and phase B is open as indicated by the shaded region in fig 2.2. In this interval, phase A winding is connected to the positive terminal of the DC supply, phase C to the negative terminal of DC supply and phase B is open. Therefore i_a=-$i_c$and i_b=0. It can be seen from fig. that the back EMF in phase A and C are equal and opposite. Therefore, in that interval (7) may be simplified as

$$V_{abbc} = V_{ab} - V_{bc} = e_{an} - 2e_{bn} + e_{cn} = -2e_{bn} \tag{2.15}$$

The difference of line voltages waveform is, thus, an inverted representation of the back EMF waveform. The EMF values would be those in a resistance, inductance, and EMF representation of the phase. It may be also be noted that the subtraction operation provides a gain of two to the EMF waveform thus amplifying it. It is again evident from figure. During this interval the back EMF e_{bn} transits from one polarity to another crossing zero. Therefore, the operation V_{ab}-V_{bc} (V_{abbc}) enables difference of the zero crossing of the phase B EMF. Similarly, the difference of the voltages V_{bcca} Enables the detection of zero crossing of phase C back EMF when phase B and C back EMFs are equal and opposite. The difference of line voltage V_{caab} waveform gives the zero crossing of phase A back EMF where phases C and B have equal and opposite back EMFs. Therefore, the zero-crossing instants of the back EMF waveforms may estimate on directly from measurements of only three terminal voltages of the motor.

While aforementioned used an ideal trapezoidal waveform, the practical induced EMF deviates from this wave shape due to its slot ripples.The validity of (8) for a practical machine is verified from experimental waveform. Real back EMF waveforms are measured and the voltage difference V_{abbc} is evaluated from the expression e_a+e_c-2_{eb} using the measured back EMF waveforms in order to verify the zero crossing instant matches.

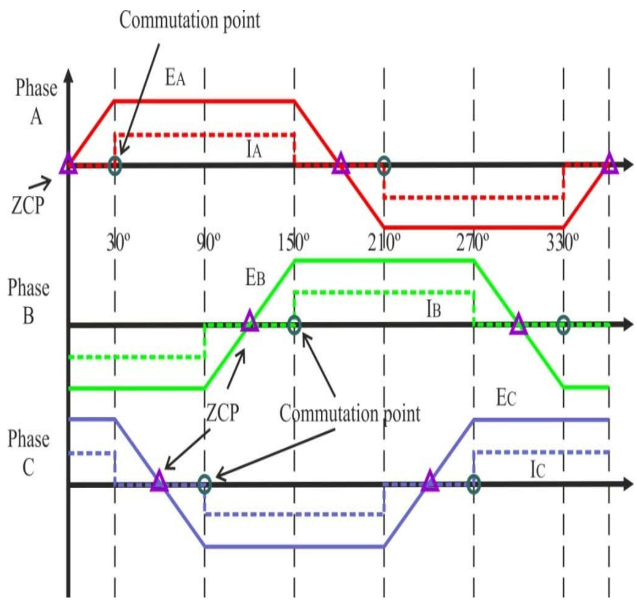

Figure 2.2: Back EMF waveforms of phase A, B and C

Fig 2.2 shows that the V_{abbc} waveform along with the back EMF waveform and the error between the two. It is evident from fig 2.2. That the V_{abbc} waveform matches well with the back EMF waveform -2_{eb} in the zero crossing region.

While the EMF waveform from fig 2.2 pertains to the machine used further in experimentation, the validity of (8) was further tested with another experimental EMF waveform published in the literature, which shows a much larger slot ripple.
The proposed sensorless methods uses this approach to estimate the zero crossing instants of the back EMF from the motor terminal voltage of the motor from which the correct communication instants are estimated.

Controller Design

A. DESIGN OF PI CONTROLLER

In a control system, in order to control the output when a state or reference value changes, a closed loop control algorithm is required. There are many control algorithms such as feed forward control, bang-bang control, proportional (P), proportional integral (PI), proportional derivative (PD), and proportional integral derivative (PID) control etc. Among all of these, the PI algorithm is the most common control algorithm used due to its simplicity and performance. The PI control algorithm computes the controlled output by calculating the proportional integral errors and summing those two components to compute the output. The control mechanism uses the current error (proportional term) and history of errors (integral term) to determine the current output.

The block diagram of the PI controller (in continuous domain) is shown in 3.5

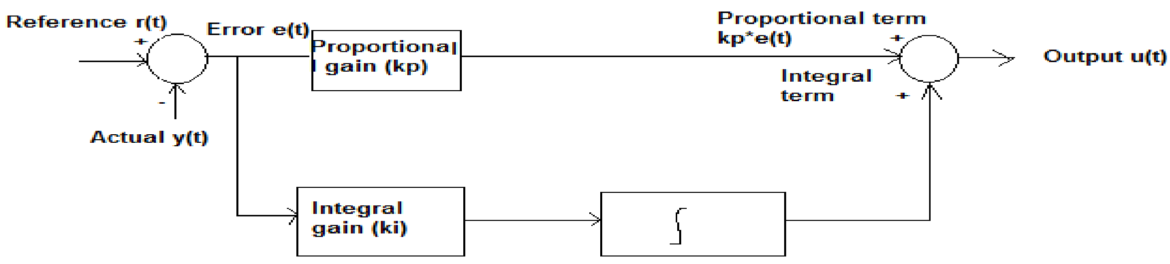

Figure 3.5 PI Controller block diagram

The mathematical model for a PI controller in a continuous domain is: $u(t) = kp * e(t) + \mathrm{ki} * \int_0^t e(\tau)\, d\tau$

(3.1)

where,

kp= Proportional gain

ki = Integral gain

e(t) = Error value (e(t) = r(t)-y(t))

r(t) = Reference input

y(t) = Actual input

u(t) = Output or the controlled variable.

Standard Form of PI Controller

For practical purposes, the above PI mathematical model is modified and used. This modified equation is known as the standard form of PI controller.

The modified equation is:

$$u(t) = kp[e(t) + \frac{1}{Ti} * \int_0^t e(\tau)\, d\tau] \quad (3.2)$$

where,

Kp (standard form) = kp (theoretical form)

$\frac{kp}{Ti}$ (standard form) = ki (theoretical form)

Ti = Integral time, a tuning parameter Ti provides a weight to the integral term so that the integral action can be independently adjusted.

In the discrete domain, the modified or standard form is written as: $(n)=Yp(n)+Yi(n)$

(3.3)

The proportional term in discrete form is:

$$Y(n)=Kp*e(n) \quad (3.4)$$

The integral term in discrete form is:

$$Yi(n) = \frac{kp*T}{Ti} * \sum_{k=o}^{n} e(k) \quad (3.5)$$

$$Yi(n) = \mathrm{ki} * \sum_{k=o}^{n} e(k) \quad (3.6)$$

where, $\frac{kp*T}{Ti}$

T= Sample time

The PI output equation in discrete form can be written as:

$$(n) = Kp * e(n) + \text{ki} * \sum_{k=o}^{n} e(k) \quad (3.7)$$

To get the desired output, the values of Kp and Ki must be chosen accordingly. This process of estimating the optimal values of Kp and Ki for a particular application is called as tuning of PI controller. Understanding the effect of Kp and Ki in the equation of a PI controller is essential for fixing the values of Kp and Ki.

Proportional Gain (Kp) Effect

The proportional component depends only on the error, which is defined as the difference between the reference input and the actual input. The proportional gain (Kp) determines the ratio of output response to the error.

In general, increasing the proportional gain increases the speed of the control system response and also decreases the steady-state error which is the final difference between reference input and actual input. However, if the proportional gain is too large, the output begins to oscillate and any further increase in Kp causes the oscillations to become larger and leads to system instability.

Integral Gain (Ki) Effect

The integral component integrates the error over time to overcome the steady-state error. Therefore, the integral response continuously increases over time unless the error is zero. However, the integral action may cause overshoot, oscillations, and instability problems if the selected integral gain (Ki) is too large. Smaller values of Ti have a stronger integral effect (since it is in the denominator of the integral gain term) on the system response.

B. Design Of Fuzzy Controller

Error (E) and Change in error (CE) are the inputs for the fuzzy controller whereas the output of the controller is change in duty cycle. The error is defined as the difference between the reference speed and actual speed, the change in error is defined as the difference between the present error and previous error and the output, duty cycle is which could be either positive or negative is added with the existing duty cycle to determine the new duty cycle. Figure shows the block diagram of fuzzy controller. The fuzzy logic controller composed of fuzzification, fuzzy rule-base, fuzzy inference engine and defuzzification.

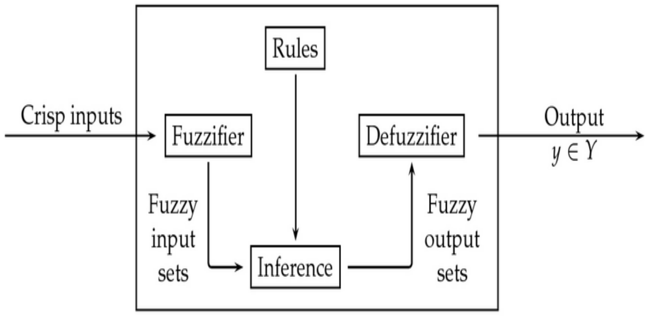

Figure 3.2: Block diagram of FLC

Fuzzification

The process of converting input/output variable to linguistic levels is termed as fuzzification. The fuzzy logic controller requires that each input/output variable which define the control surface be expressed in fuzzy set notations using linguistic levels. The linguistic values of each input and output variables divide its universe of discourse into adjacent intervals to form the membership functions. The member value denotes the extent to which a variable belong to a particular level and depends upon the consequence and IF…THEN… rule strength. The rule strength will be computed by fuzzy "AND" operation of inputs.

Inference

The behavior of the control surface which relates the input and output variables of the system governed by a set of rules. A typical value would be if x is A then y is B when a set of input variables are read each of the rule that has any degree of truth in its premise is fired and contributes to the forming of the control surface by approximately modifying it. When all the rules are fired, the resulting control surface is expressed as a fuzzy set to represent the constraints output. This process is termed as inference.

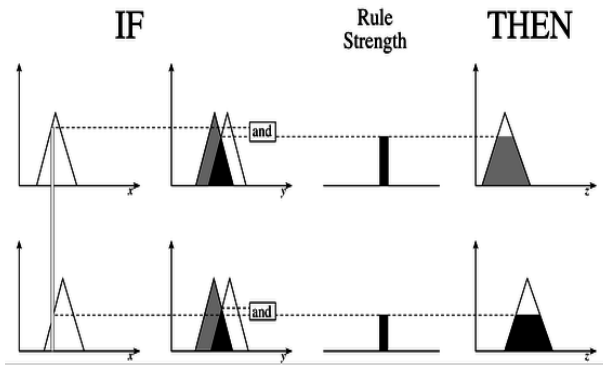

Figure 3.3: Fuzzy Inference

Defuzzification

Defuzzification is the process of conversion of fuzzy quantity into crisp quantity. There are seven methods available for defuzzification. The most commonly used defuzzification techniques are:

1. **Center of Mass:** This technique takes the output distribution and finds its center of mass to come up with one crisp number. This is computed as

$$\frac{\sum_{j=1}^{q} Zjuc(Zj)}{\sum_{j=1}^{q} uc(Zc)}$$

Where z is the center of mass and $u_c$is the membership in class c at value $z_{j.}$

2. Mean of Maximum: This technique takes the output distribution and finds its mean of maxima to come up with one crisp number. This is computed as follows.

$$\sum_{j=1}^{l} \frac{zj}{l}$$

Where z is the mean of maximum. $z_j$is the point at whichthe membership function and l is the number of times the output distribution reaches the maximum level.

In this paper Center of mass method is used as defuzzifier.The 49 rules formulated for the proposed fuzzy logic control system are listed below.

E/CE	**NB**	**NM**	**NS**	**Z**	**PS**	**PM**	**PL**
NB	NB	NB	NB	NB	NM	NS	Z
NM	NB	NB	NB	NM	NM	Z	PS
NS	NB	NB	NM	NS	Z	NS	PM
Z	NB	NM	NS	Z	NS	PM	PB
PS	NM	NS	Z	PS	PS	PS	PS
PM	NS	Z	PS	PM	PB	PB	PB
PL	Z	PS	PM	PB	PB	PB	PB

Simulation and Results

The Fig. 4.1 shows the simulation circuit of the proposed sensorless control of BLDC servomotor.

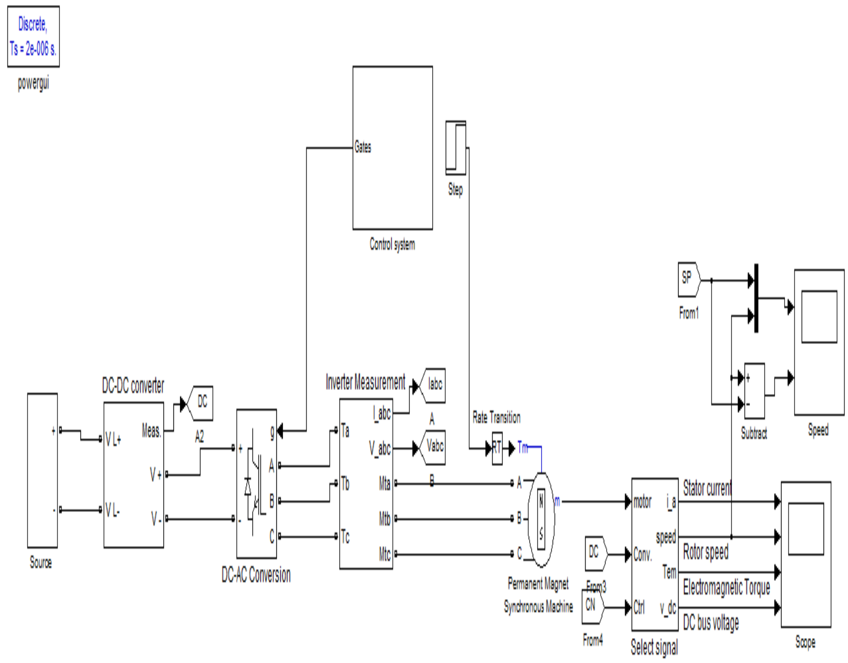

Figure4.1: Simulation diagram

The simulation results includes variation of different parameters of BLDC motor like change in reference speed, change in load torque. Figure shows the stator current, rotor speed, Electromagnetic torque and dc bus voltage waveforms.

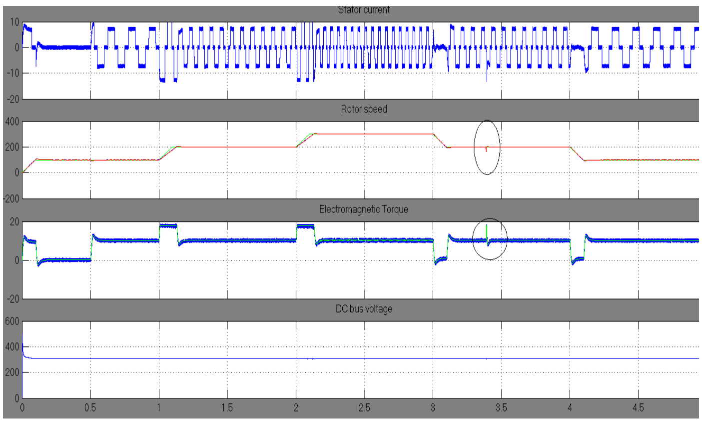

Figure4.2: Simulation output of PI Controller (Load torque1)

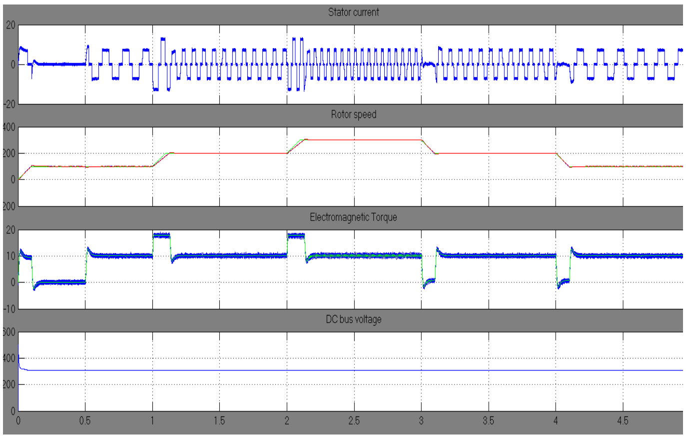

Figure4.3: Simulation output of Fuzzy Controller (Load torque 1)

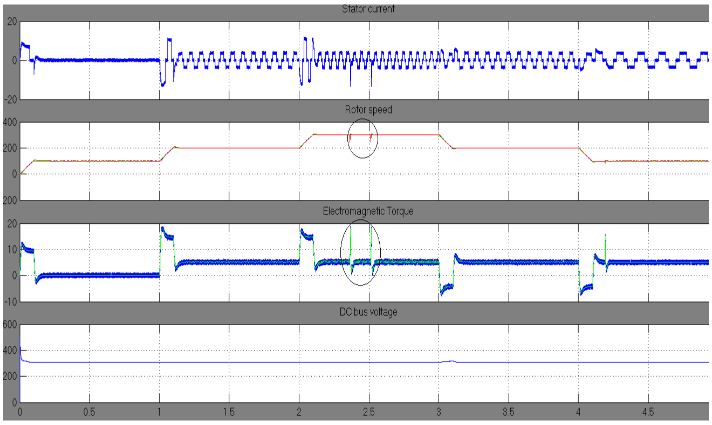

Figure 4.4: Simulation output of PI Controller (Load torque1)

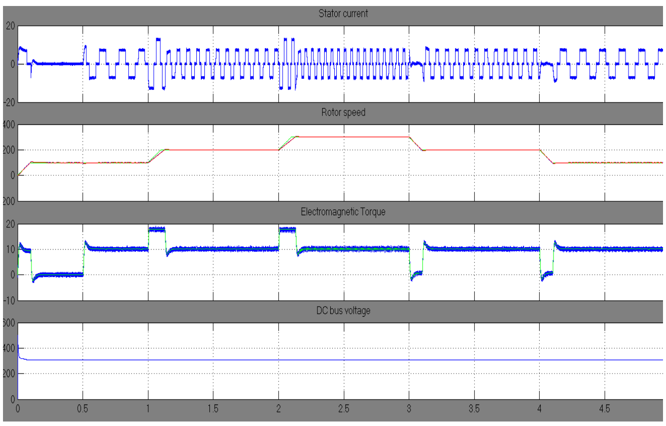

Figure 4.5: Simulation output of Fuzzy Controller (Load torque 2)

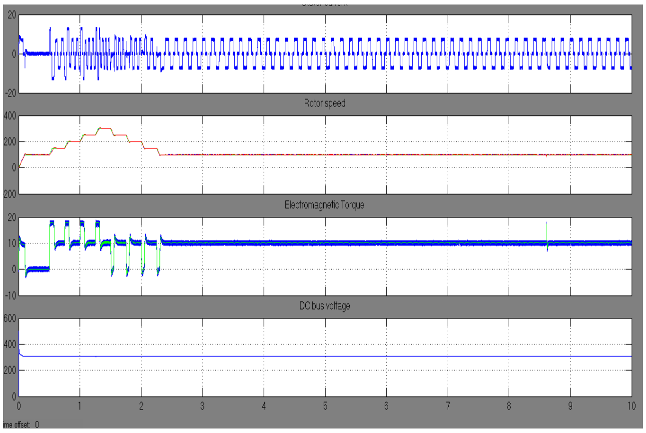

Figure4.6: Simulation output of PI Controller (Reference speed)

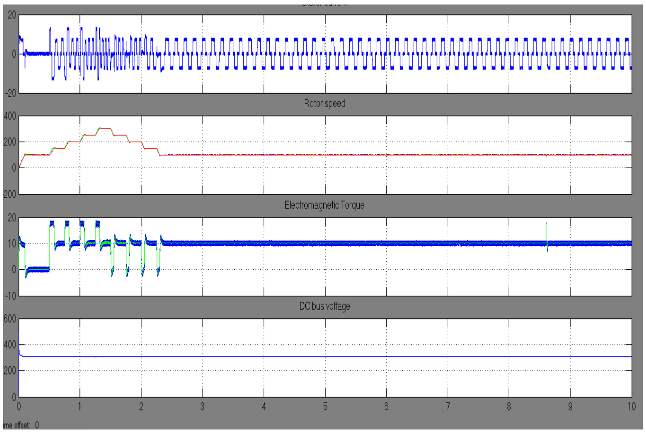

Figure4.7: Simulation output of PI Controller (Reference speed)

Conclusion

The PI and fuzzy control techniques are simulated for sensorless BLDC servo motor drive system. The speed response of fuzzy controller based sensorless BLDC servomotor drive is similar to speed response of PI controller based sensorless BLDC servomotor drive when system parameters are constant. However, the speed response of fuzzy controller based sensorless BLDC servomotor drive is found to be better than speed response of PI controller based sensorless BLDC servomotor drive system when system parameter changes. Therefore, PI controller based sensorless BLDC servomotor drive failed to provide improved performance under performance variations of the system. But experimental results clearly shows that fuzzy controller based sensorless BLDC servomotor drive can provide an improved speed response with consistently same rise time, and settling time when the system subjected to load disturbance, parameter variations, and step change in referencespeed. Since fuzzy control system is easy to design and implement, effective in dealing with the uncertainties and parameter variations, and has better overall performance.

REFERENCES

[1] Bhim Singh, B P Singh, (Ms) K Jain, “Implementation of DSP Based Digital Speed Controller for Permanent Magnet Brushless dc Motor”This paper (redrafted) was received on July 3, 2002. Written discussion on thispaper will be received till September 30, 2003.*IE(I) Journal-EL, Vol 84, June 2003*

[2] José Carlos Gamazo-Real , Ernesto Vázquez-Sánchez and Jaime Gómez-Gil,“ Speed Control of Brushless DC Motors Using Sensorless Techniques and Application Trends”in ISSN 1424-8220 *Received: 10 June 2010; in revised form: 30 June 2010 / Accepted: 5 July 2010 / Published:* 19 July 2010

[3] B.Maheshkumar, G.Ravi and R.Chakrabarti, “Sensorless speed control of Brushless DC motor with fuzzy based Estimation”,inIranian Journal of electrical and Computer Engineering, vol.8, No 2, summer Fall 2009

[4] P.Pillai and R.Krishnan, “Modeling, simulation, and analysis of permanent magnet motor drives”in part ii: The brushless dc motor drive,”*IEEE Trans. Ind. Appl.*, vol. 25, no. 2, pp. 274–279, Mar./Apr. 1989.

[5] R.Shanmugasundaram, K.MohammedZakariah, N.Yadaiah, “ Implementation and Performance analysis of Digital controllers for Brushless DC Motor Drives”in IEEE/ASME Transactions on Mechatronics, Vol.19, No 1, February 2014.

[6] R.Shanmugasundram, K.M. Zakariah, and N.yadaiah, “Low cost high performance brushless dc motor drive for speed control applications,” in Proc. IEEE Int.Conf.Asd.RecentTechnolo.Commn, comput, Kottayam, Inida, Oct. 27-28,2009, pp. 456-460.

[7] R.Shanmugasundram, K.M. Zakariah, and N.yadaiah, “ Digital implementation of fuzzy logic controller for wide range speed control of brushless dc motor” in proc.IEEE Int. Conf. Veh. Electron.Safety,Pune, India, Nov. 10-12,2009,pp.119-124.

[8] R.Somanatham, P.V.N.Prasad, A.D.Rajkumar, “Modeling and Simulation of sensorless control of PMBLDC Motor using zero-crossing Back EMF Detection method”in SPEEDAM 2006

[9] R.Krishnan, Permanent Magnet Synvhrounos and Brushless Dc Motor Drives: Theory, Operation, Performance, Modeling , Simulation, Analysis, and design- Part 3, Permanent Magnet Brushless DC Machines and their Control. Boca Raton, FL: CRC Press, 2009, pp.451-563.